Journal of Applied Toxicology

WILEY

Journal of AppliedToxicology

RESEARCH ARTICLE

Pulmonary Side Effects Associated With Abemaciclib the Antibreast Cancer Drug in Female Mice

Wajdan S. Alqahtani[1] | Badr A. Aldahmash[1] | Doaa M. Elnagar[1] | Ahmed M. Rady[1] | Elham M. Alzahrani[1] | Waad Alsubaie[1] | Shahad Gannamah[1] | Saad Alkahtani[1] | Mobarak S. Al Mosallam[1] | Amjad Khan[2] | Savarimuthu Ignacimuthu[3] | Pathalam Ganesan[3]

[1]Department of Zoology, College of Science, King Saud University, Riyadh, Saudi Arabia | [2]Kangbuk Samsung Hospital, Samsung Medical Center, School of Medicine, Sungkyunkwan University (SKKU) Seoul, Seoul, South Korea | [3]Interdisciplinary Research Centre in Biology, Xavier Research Foundation, St Xaviers College (Affiliated to Manonmaniam Sundaranar University), Tirunelveli, Tamil Nadu, India

Correspondence: Pathalam Ganesan (sundarganeshps@gmail.com)

Received: 2 September 2025 | **Revised:** 23 September 2025 | **Accepted:** 25 September 2025

Funding: The authors express their sincere appreciation to the Ongoing Research Funding Program, King Saud University, Riyadh, Saudi Arabia (ORF-2025-214).

Keywords: abemaciclib drug | adiponectin | DMBA | lung toxicity | mammary carcinoma

ABSTRACT

This study investigated the potential lung-related side effects of abemaciclib in virgin female mice. Animals were divided into four groups: Group 1 (control) received clean drinking water; Group 2 received abemaciclib orally (50 mg/kg/day) for 28 days; Group 3 was given a single dose of 7,12-dimethylbenz(a)anthracene (DMBA, 50 mg/kg) to induce mammary carcinoma; and Group 4 received DMBA followed by abemaciclib treatment (50 mg/kg/day for 28 days) starting 10 days post-induction. Biochemical, histopathological, and immunohistochemical analyses were performed, including hormonal assays, liver enzymes, kidney biomarkers, oxidative stress markers (malondialdehyde [MDA] and catalase [CAT]), and adiponectin/TNF-α expression. DMBA administration significantly elevated estrogen, progesterone, liver enzymes, kidney biomarkers, and MDA, while reducing CAT activity. Abemaciclib treatment decreased estrogen and progesterone levels but further increased liver enzymes, kidney biomarkers, MDA, and reduced CAT. Breast histopathology in the DMBA group revealed invasive ductal adenocarcinoma with strong desmoplastic reaction, whereas abemaciclib treatment reduced tumor size and stromal reaction. Lung tissue of the DMBA group showed severe inflammation, epithelial hyperplasia, and dysplasia. Abemaciclib-treated lungs exhibited interstitial inflammation, fibrosis, and vascular thrombosis, indicating aggravated pulmonary changes. Immunohistochemically, DMBA reduced adiponectin expression in the breast, which was restored by abemaciclib. Conversely, TNF-α expression in the lung was increased by DMBA and further elevated after abemaciclib. In summary, DMBA successfully induced mammary carcinoma and lung toxicity. While abemaciclib reduced breast tumor burden, it was associated with exacerbated pulmonary toxicity, suggesting the need for careful evaluation of its lung-related side effects.

1 | Introduction

Cancer is the second leading cause of mortality worldwide, following cardiovascular diseases. In 2008, malignant neoplasms were responsible for approximately eight million deaths globally, a number projected to rise to 11 million by 2030 (Momenimovahed and Salehiniya 2019). Cancer poses a significant threat to public health across all human societies. Among men, the most commonly diagnosed cancers include those of the prostate, lung, colorectum, and urinary bladder, whereas in women, breast and uterine cancers are most prevalent. These data indicate that prostate cancer in men and

breast cancer in women account for a substantial proportion of all cancer cases by gender (Hassanpour and Dehghani 2017).

Breast cancer is the most frequently diagnosed malignancy worldwide, with its incidence and disease burden rising steadily over recent decades (Arnold et al. 2022). It is the most common cancer among women, accounting for approximately 30% of all cancer diagnoses annually, excluding skin cancers. Furthermore, it is the second leading cause of cancer-related death among women (Cakcak et al. 2023). Although breast cancer occurs globally, there are significant regional differences in incidence, mortality, and survival rates. These disparities may be attributed to multiple factors, including population demographics, lifestyle, genetic predisposition, and environmental influences. The increasing prevalence of breast carcinoma is largely driven by changing risk factors (Momenimovahed and Salehiniya 2019).

Breast cancer is categorized into five stages based on the TNM staging system—Tumor (T), Node (N), and Metastasis (M)—which considers tumor size, lymph node involvement, and the presence of distant metastasis (CRUK 2023). In addition to staging, breast cancer is graded histologically into three levels based on cellular differentiation and malignancy. Breast cancers are further classified based on hormone receptor (HR) status, depending on the presence or absence of estrogen (ER) and progesterone (PR) receptors on tumor cells (ACS 2021).

Abemaciclib is a small-molecule drug used in the treatment of HR+/HER2− breast cancer. Its chemical formula is $C_{28}H_{36}F_2N_8O_3S$, and it is known as the mesylate salt of N-[5-[(4-ethylpiperazin-1-yl)methyl]pyridin-2-yl]-5-fluoro-4-(7-fluoro-2-methyl-3-propan-2-ylbenzimidazol-5-yl)pyrimidin-2-amine; methanesulfonic acid (NCI 2022). In October 2021, the US Food and Drug Administration (FDA) approved abemaciclib (marketed as Verzenio by Eli Lilly and Company) as the first and only CDK4/6 inhibitor for adjuvant treatment in adults with HR+, HER2−, node-positive breast cancer (Food and Drug Administration 2021; Royce et al. 2022). Abemaciclib targets cyclin D1–CDK4 and cyclin D3–CDK6 pathways, thereby inhibiting cell cycle progression and exerting anticancer effects (NCI 2022). Abemaciclib reduced tumor growth in mice by inhibiting CDK4/6-mediated phosphorylation of the Rb protein and suppressing E2F activity, resulting in G1 cell-cycle arrest and the subsequent induction of apoptosis in tumor cells (Corona and Generali 2018). Given its widespread use in breast cancer therapy, the present study was designed to evaluate the potential side effects of abemaciclib on lung tissue in female mice.

2 | Materials and Methods

2.1 | Materials

Abemaciclib, with the commercial name Verzenio, was purchased from Eli Lilly and Company, Riyadh, Saudi Arabia.

2.2 | Experimental Animals

Forty virgin female Swiss Albino mice, aged 14 weeks and weighing 25 ± 5 g, were obtained from the Animal House Facility, College of Science, King Saud University, Riyadh, Saudi Arabia. The animals were housed in clean cages under standard environmental conditions (25°C, 12-h light/dark cycle) with free access to a balanced diet and clean drinking water.

2.3 | Experimental Design and Sample Collection

The animals were randomly divided into four groups, with 10 mice in each group:

- **Group 1 (Control)**: Received no treatment (drinking water only).
- **Group 2 (Abemaciclib)**: Received a daily oral dose of 50 mg/kg abemaciclib for 28 days.
- **Group 3 (Tumor Group)**: Received a single dose of 50 mg/kg 7,12-dimethylbenz[a]anthracene (DMBA; Sigma, Taufkirchen, Germany) injected into the breast fat pad to induce mammary tumors.
- **Group 4 (DMBA + abemaciclib)**: Received DMBA as in Group 3, followed by abemaciclib treatment (50 mg/kg orally, once daily) starting 10 days after tumor induction, and continued for 4 weeks.

At the end of the experiment, animals were euthanized under carbon dioxide (CO_2) anesthesia. Blood samples were collected via cardiac puncture and transferred into EDTA-coated tubes for complete blood count analysis.

Breast and lung tissues from all groups were excised and fixed in 10% formalin for histopathological and immunohistochemical evaluation. Liver and ovary tissues were collected, homogenized in ice-cold phosphate-buffered saline (PBS) at a ratio of 1:3 for 3 min, and then centrifuged twice at 3000 × g for 20 min. The resulting supernatant was filtered and stored at −80°C for subsequent biochemical analyses.

2.4 | Breast and Lung Index

Each mouse was individually weighed, and the lungs and breast tissues were excised and weighed. The breast and lung indices were calculated by dividing the organ weight by the body weight and multiplying by 100:

$$\text{Organ Index} = \left(\frac{\text{Organ Weight (g)}}{\text{Body Weight (g)}}\right) \times 100$$

2.4.1 | Biochemical Analysis

2.4.1.1 | Estimation of Female Hormones. Estrogen and progesterone levels were measured in homogenized ovarian tissue using enzyme-linked immunosorbent assay (ELISA) kits (Elab Science Company, Texas, USA), following the manufacturer's protocols.

2.4.1.2 | Determination of Liver Enzymes. Liver homogenate supernatants were used to assess the activity of liver enzymes—alanine transaminase (ALT), aspartate

aminotransferase (AST), and alkaline phosphatase (ALP)—using commercial kits provided by Elabscience (Texas, USA), in accordance with the manufacturer's instructions.

2.4.1.3 | Estimation of Kidney Biomarkers. Levels of uric acid, urea, and creatinine were quantified from liver homogenate supernatants using commercial kits (Elabscience, Texas, USA), following the respective manufacturer protocols.

2.4.1.4 | Determination of Oxidative Stress Biomarker (MDA) and Antioxidant Activity (Catalase [CAT]). Malondialdehyde (MDA) and catalase (CAT) levels in liver homogenates were determined using commercial kits supplied by Elabscience (Texas, USA).

2.4.2 | Histopathological Analysis

Breast and lung tissues were fixed in 10% formalin, dehydrated through ascending grades of alcohol, embedded in paraffin, sectioned at 6 μm thickness, and dried. Sections were stained with hematoxylin and eosin (H&E), Masson's Trichrome (M.Tr), and Periodic Acid–Schiff (PAS) stain (for lung tissues). Photomicrographs were captured using a Nikon microscope (Nikon, Tokyo, Japan), and image analysis was performed using Fiji software (FNPF Place, Suva, Fiji) to calculate the area percentage and optical density (OD), using the formula:

$$\mathrm{OD} = \log\left(\frac{\mathrm{Max}}{\mathrm{Mean}}\right) \times 100$$

Breast tissue sections were graded according to the Nottingham histological score (Takahashi et al. 2020):

- Grade 0 (score 0): Normal tissue
- Grade 1 (score 3–5): Low-grade carcinoma
- Grade 2 (score 6–7): Intermediate-grade carcinoma
- Grade 3 (score 8–9): High-grade carcinoma

Lung sections were evaluated using the pulmonary histopathological scoring system described by Passmore et al. (2018).

2.4.3 | Immunohistochemistry

Immunohistochemical detection of adiponectin in breast tissue and TNF-α in lung tissue was performed using the Avidin–Biotin Complex (ABC) method. Paraffin-embedded sections were deparaffinized, rehydrated, and subjected to antigen retrieval using Tris-EDTA buffer (pH 9) in a microwave for 7 min. After washing with PBS (three times), endogenous peroxidase activity was blocked using hydrogen peroxide, followed by incubation with a protein blocking solution. Sections were then incubated with primary antibodies, followed by biotinylated secondary antibodies (30 min), and subsequently with Streptavidin–HRP (10 min). Finally, sections were developed using DAB substrate for 30 min. All steps were carried out in a humidity chamber. Antibodies were obtained from Santa Cruz Biotechnology Inc., California, USA (IMMUNE SYSTEM SC-2018). Images were analyzed using Fiji software to calculate area percentage and optical density (OD), using the same formula as above.

2.4.4 | Statistical Analysis

Data are presented as mean ± standard error of the mean (SEM). Statistical differences between control and treated groups were analyzed using one-way analysis of variance (ANOVA). Differences were considered statistically significant at $p \leq 0.05$. Analyses were conducted using SPSS software version 16.0 (IBM, Armonk, NY, USA).

3 | Results

3.1 | Breast and Lung Index

In the breast index, the abemaciclib-treated group showed no significant change compared with the control group. However, the tumor group showed a significant increase relative to the control ($p \leq 0.05$). The tumor group treated with abemaciclib exhibited a non-significant decrease compared with the tumor group. Regarding the lung index, both the abemaciclib-treated group and the tumor group showed a significant increase compared with the control ($p \leq 0.05$). Additionally, the tumor group treated with abemaciclib displayed a significant increase in lung index compared with the tumor group alone (Figure S1).

3.2 | Abemaciclib Inhibits Estrogen and Progesterone Levels

Estrogen levels were significantly decreased in the abemaciclib-treated group compared with the control group ($p \leq 0.05$), whereas the tumor group showed a significant increase. The tumor group treated with abemaciclib demonstrated a significant decrease in estrogen levels compared with the tumor group. Progesterone levels were significantly increased in both the abemaciclib-treated and tumor groups relative to the control group ($p \leq 0.05$). However, the tumor group treated with abemaciclib showed a significant reduction in progesterone levels compared with the tumor group (Figure S2).

3.3 | Liver Enzyme Activity (ALT, AST, ALP)

Levels of ALT, AST, and ALP were significantly elevated in both the abemaciclib-treated and tumor groups compared with the control ($p \leq 0.05$). Furthermore, the tumor group treated with abemaciclib exhibited significantly higher levels of these liver enzymes compared with the tumor group alone (Figure S3).

3.4 | Kidney Biomarkers

Uric acid levels were significantly increased in both the abemaciclib-treated and tumor groups compared with the control. However, the tumor group treated with abemaciclib showed no significant change in uric acid levels compared with the tumor group. Urea levels were significantly elevated in the abemaciclib-treated

and tumor groups compared with the control, while the tumor group treated with abemaciclib showed a significant decrease in urea compared with the tumor group. Creatinine levels were significantly decreased in the abemaciclib group compared with the control, whereas the tumor group exhibited a significant increase. No significant difference was observed between the tumor and tumor + abemaciclib groups (Figure S4).

3.5 | Oxidative Stress and Antioxidant Markers

MDA levels were significantly increased in both the abemaciclib-treated and tumor groups relative to the control ($p \leq 0.05$). However, the tumor + abemaciclib group did not differ significantly from the tumor group. CAT activity was significantly decreased in both the abemaciclib-treated and tumor groups compared with the control. No significant difference in CAT activity was observed between the tumor and tumor + abemaciclib groups (Figure S5).

3.5.1 | Histopathological Analysis

3.5.1.1 | Abemaciclib Reduces Mammary Carcinoma Formation. Breast tissue in the control group appeared normal with well-formed mammary glands and ducts (Figure 1A). The abemaciclib-treated group showed mild tissue congestion (Figure 1B). The tumor group (DMBA only) exhibited extensive invasive tubular mammary adenocarcinoma with pleomorphic cancer cells forming carcinoma nests (Figure 1C). The tumor group treated with abemaciclib displayed a reduced incidence of carcinoma (Figure 1D). Masson's Trichrome staining showed normal collagen distribution in the control and abemaciclib groups (Figure 2A,B), with significantly lower area percentage and optical density in the abemaciclib group compared with control (Figure S6). In contrast, the tumor group exhibited marked collagen deposition and desmoplastic stroma (Figure 2C), with significantly increased area percentage and optical density. Abemaciclib treatment in the tumor group reduced collagen deposition and desmoplasia significantly compared with the untreated tumor group (Figure 2D; Figure S6). All images were graded using the Nottingham histological score (Table 1).

3.5.1.2 | Adverse Effects of Abemaciclib on Lung Tissue. Lung tissue from the control group showed normal architecture, including well-opened bronchioles and alveolar sacs (Figure 3A). The abemaciclib group showed thickened interalveolar septa and leukocytic infiltration (Figure 3B). The tumor group displayed inflammatory cell accumulation, septal thickening, and alveolar obstruction (Figure 3C). The tumor + abemaciclib group exhibited severe alterations including bronchiolar epithelial dysplasia and dense inflammatory infiltration (Figure 3D).

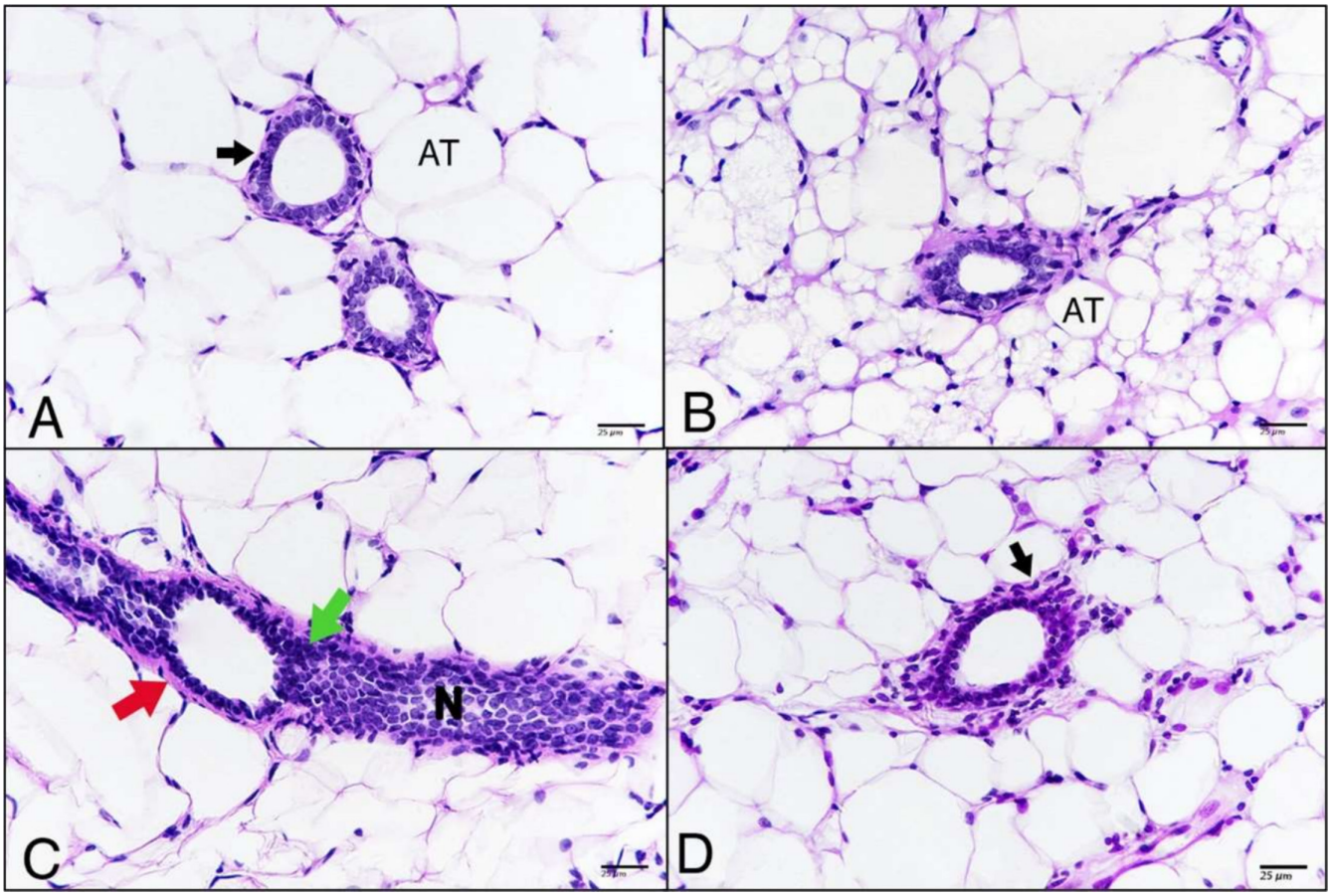

FIGURE 1 | Photomicrographs of breast tissue (A) untreated control showing normal appearance, adipose tissue (AT), gland (black arrow), (B) breast of mice treated with 50 mg/kg of abemaciclib (C) breast of tumor group atypical proliferative cells in the ductal lumen (green arrow), carcinoma nests (N), desmoplastic stroma (red arrow), (D) breast of tumor group treated with 50 mg/kg of abemaciclib showing less carcinoma incidence (black arrow) (H&E—400×).

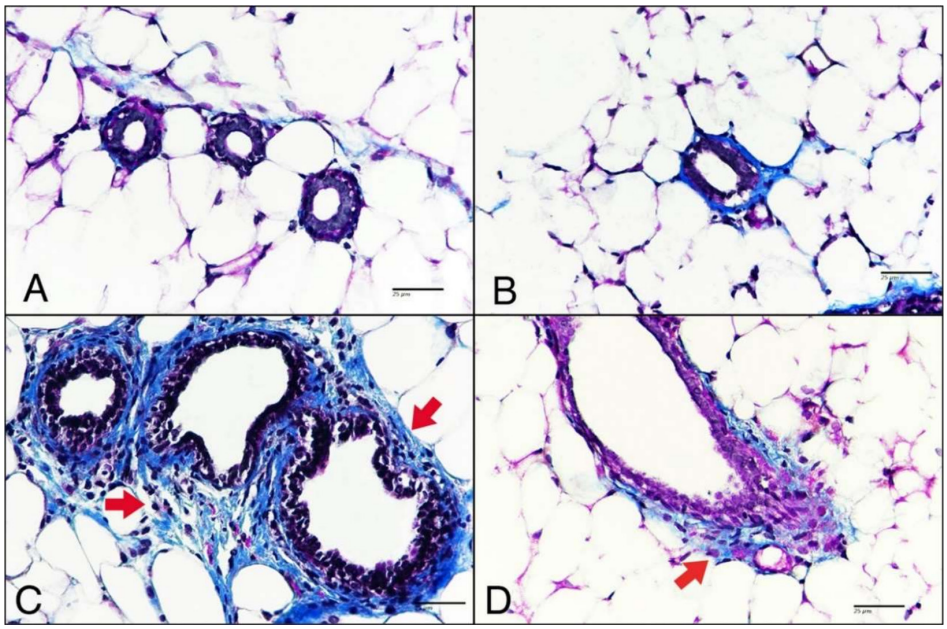

FIGURE 2 | Photomicrographs of breast tissue (A) untreated control showing no fibrosis, (B) breast of mice treated with 50 mg/kg of abemaciclib (C) breast of tumor group revealing intense desmoplastic stroma (red arrow), (D) breast of tumor group treated with abemaciclib 50 mg/kg posting less desmoplastic reaction (red arrow) (M.tr.—400×).

TABLE 1 | Nottingham histopathological score showing reduced effect of abemaciclib on mammary adenocarcinoma.

Group	Grade	Score
Control	0	0
Abc 50	0	0
Tumor (DMBA)	2	7
T + Abc 50	1	4

Masson's Trichrome staining of the lungs revealed no collagen deposits in the control (Figure 4A), while the abemaciclib group showed excessive collagen and ECM deposits (Figure 4B), with increased percentage and optical density (Figure S7). The tumor group displayed bronchiolar destruction and high collagen deposition (Figure 4C), with significantly increased area and optical density. The tumor + abemaciclib group exhibited high fiber content with insignificant changes in area percentage but increased optical density compared with the tumor group (Figure 4D; Figure S7).

PAS staining showed normal ECM distribution and absence of hyaline membranes in the control (Figure 5A). The abemaciclib group exhibited hyaline membranes and mucus accumulation (Figure 5B), with high PAS area percentage and optical density (Figure S8). The tumor group also showed hyaline membrane accumulation (Figure 5C), with high area percentage but lower optical density. The tumor + abemaciclib group displayed similarly high hyaline content, with increased optical density and no significant change in area percentage compared with the tumor group (Figure 5D; Figure S8). All sections were scored accordingly (Table 2).

3.6 | Immunohistochemistry Analysis

3.6.1 | Abemaciclib Enhances Adiponectin Expression in Breast Tissue

Adiponectin expression was intense in the control group (Figure 6A) and remained strong in the abemaciclib-treated group (Figure 6B), with no significant changes in area percentage or optical density (Figure S9). In contrast, the tumor group showed reduced adiponectin expression (Figure 6C), while the tumor + abemaciclib group exhibited significantly enhanced expression, with increased area percentage and optical density compared with the tumor group (Figure 6D; Figure S9).

3.6.2 | Abemaciclib Increases TNF-α Expression in Lung Tissue

TNF-α expression was weak in the control group (Figure 7A), but increased in the abemaciclib-treated group (Figure 7B), with significantly higher area percentage and optical density ($p \leq 0.05$) (Figure S10). Both the tumor and tumor + abemaciclib groups showed strong TNF-α expression (Figure 7C,D). While the tumor + abemaciclib group had no significant change in area percentage compared with the tumor group, it exhibited a significant increase in optical density (Figure S10).

4 | Discussion

In the present study, DMBA (7,12-dimethylbenz[a]anthracene), an aromatic chemical carcinogen, was used to induce mammary carcinoma. DMBA has been widely employed in experimental models as a potent chemical tumor inducer,

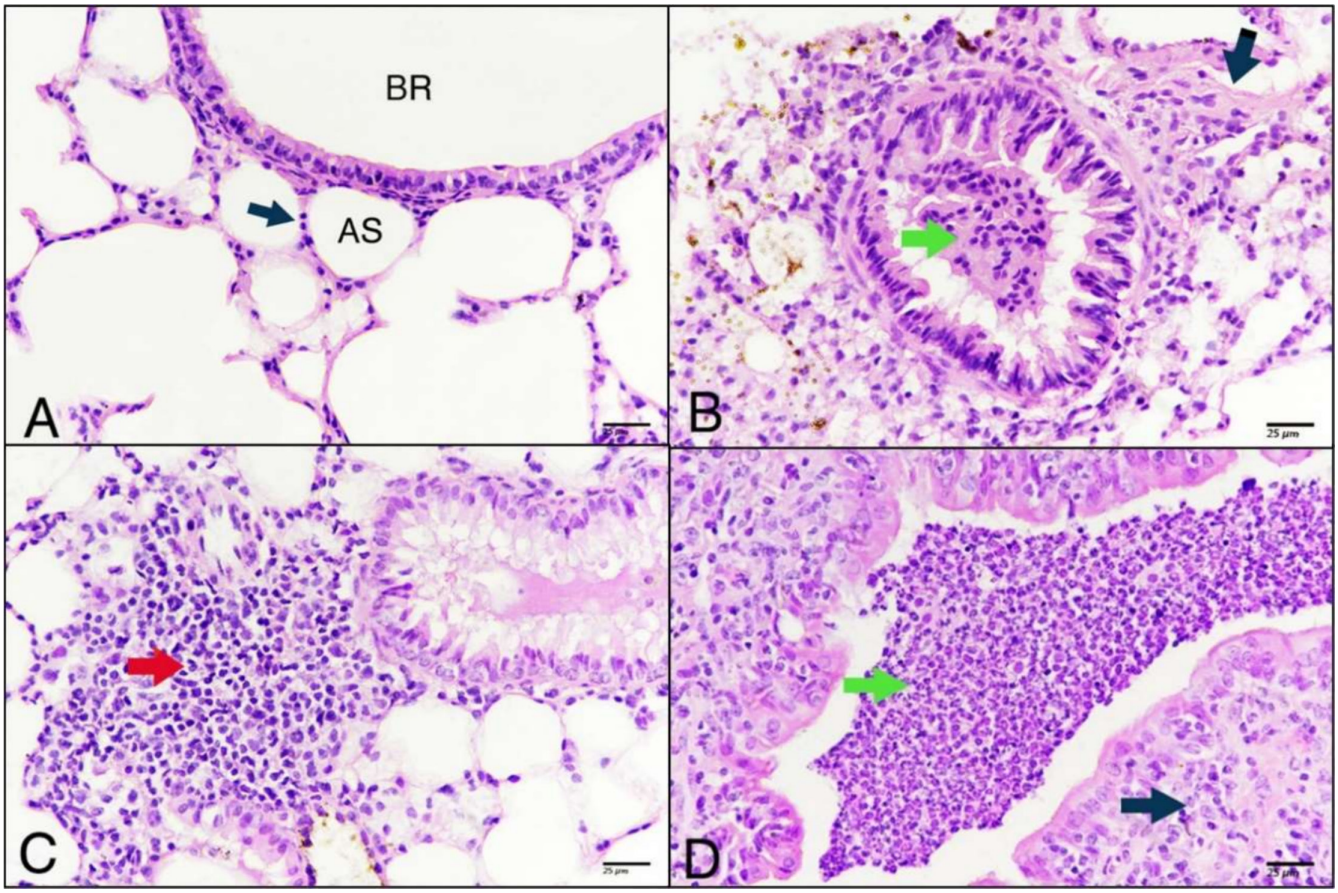

FIGURE 3 | Photomicrographs of mice lung stained with H&E. (A) Untreated control lung showing normal pulmonary view, bronchiole (BR), alveolar sac (AS), interalveolar septum (black arrow), (B) lung treated with abemaciclib 50 mg/kg showing infiltrative cells blocked bronchiole (green arrow) and thickened interalveolar septa (black arrow), (C) lung of tumor mice displaying infiltrative cells (red arrows), (D) lung of tumor group treated with abemaciclib 50 mg/kg showing dysplasia interalveolar septum (black arrow), high infiltrative cells blocked bronchiole (green arrow) (H&E—400×).

particularly for mammary carcinoma in laboratory animals (Buque et al. 2021; Corso and Acco 2018). Mechanistically, DMBA functions as a procarcinogen undergoes metabolic activation within breast tissue to form DMBA-3,4-diol-1,2-epoxide (DMBA-DE), a highly reactive intermediate. DMBA-DE disrupts redox homeostasis and triggers oxidative stress. The resulting reactive oxygen species (ROS) inflict damage on cellular DNA and cell cycle proteins, potentially leading to uncontrolled cell proliferation and tumor formation. The increasing incidence of estrogen receptor-positive (ER+) breast cancers further contributes to enhanced tumor cell proliferation (Hamza et al. 2022; Ma et al. 2018). In the current study, the DMBA-treated group exhibited a high incidence of mammary adenocarcinoma, consistent with previously reported findings.

Mechanistically, DMBA-induced tumorigenesis was associated with disruptions in signaling pathways regulating proliferation and survival. This was evidenced by an increased breast index, reflecting enhanced mammary tissue growth and hyperplasia, likely driven by DMBA-mediated DNA damage and impaired cell-cycle control (Alanazy et al. 2021; Hendi et al. 2020). Consistent with these findings, the present study observed a significant increase in the breast index of the DMBA-induced tumor group, likely due to congested blood vessels and a pronounced desmoplastic reaction, reflecting stromal remodeling in response to tumorigenesis. Interestingly, the abemaciclib-treated tumor group also exhibited an elevated breast index, which could be attributed to persistent breast tissue congestion, suggesting that while abemaciclib inhibits tumor cell proliferation, it may not immediately reverse tumor-associated stromal or vascular changes. Furthermore, previous studies have reported that DMBA-induced mammary carcinoma can elevate the lung index (Patel and Shah 2021) and that DMBA exposure can result in a high incidence of differentiated lung adenocarcinoma (Duro de Oliveira et al. 2013). In agreement with these reports, the current study found an increased lung index in the tumor group, possibly due to excessive accumulation of inflammatory cells, vascular congestion, and extracellular matrix deposition, leading to lung enlargement. Notably, both the tumor group treated with abemaciclib and the abemaciclib-only group showed a significant increase in lung index, likely resulting from inflammatory cell infiltration and alveolar sac blockage.

Moreover, DMBA-induced mammary carcinoma is known to elevate the levels of female sex hormones, particularly estrogen and progesterone (Alghamdi et al. 2024). In ER + breast cancer, estrogen activates ER signaling, promoting cyclin D expression

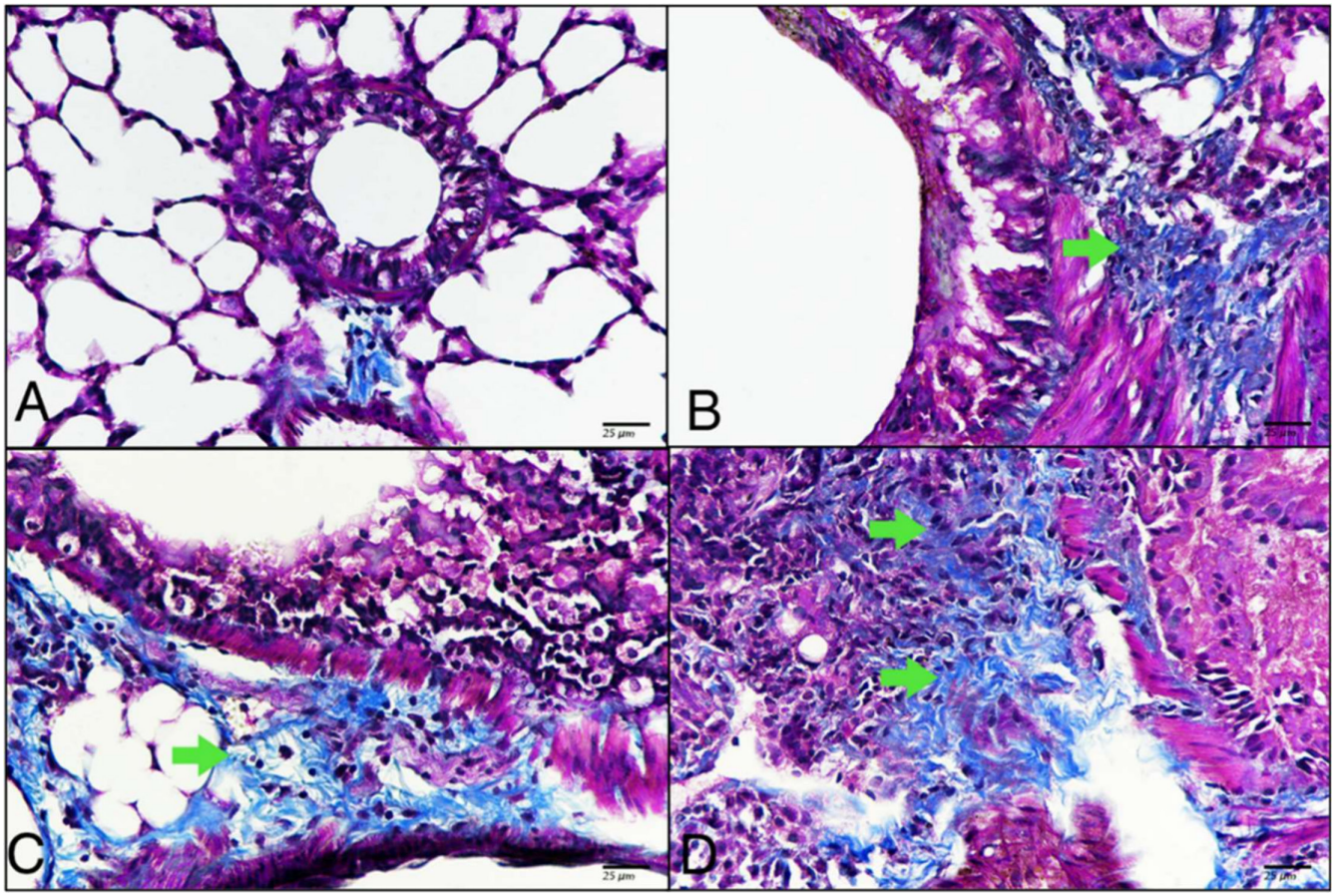

FIGURE 4 | Photomicrographs of mice lung stained with Masson's trichrome. Key: (A) Untreated control lung showing no collagenous depositions, (B) lung treated with abemaciclib 50 mg/kg showing heavy depositions of collagenous fibers (green arrow), (C) lung of tumor group displaying depositions of collagenous fibers (green arrows), (D) lung of tumor group treated with abemaciclib 50 mg/kg showing high depositions of fibers (green arrow) (Masson's trichrome—400×).

and subsequent CDK4/6 activation, which drives uncontrolled cellular proliferation. CDK4/6, as a key component of this pathway, representing a therapeutic target; its inhibition has been shown to suppress the progression of ER + breast cancer (Huang et al. 2022). In this study, a single injection of DMBA into the breast fat pad led to mammary carcinoma with a significant rise in estrogen and progesterone levels, indicating a hormone-dependent tumor. Treatment with abemaciclib effectively reduced the levels of both hormones in the tumor group. DMBA injection resulted in a significant increase in liver enzyme activity, indicating hepatic damage, as previously reported by Dakrory et al. (2015). This aligns with the present findings, where DMBA-induced breast cancer led to elevated levels of ALT, AST, and ALP, likely due to hepatocellular injury and the subsequent leakage of these enzymes into the bloodstream. Liver injury following administration of the CDK4/6 inhibitor abemaciclib has been attributed to its potential inhibition of the bile salt export pump (BSEP), a key transporter in bile acid excretion, or alternatively to an abemaciclib-induced autoimmune hepatic response (Taniguchi et al. 2022). In the current study, liver enzyme levels in the tumor group significantly increased after abemaciclib treatment, suggesting further hepatic damage.

DMBA exposure has also been reported to cause marked histological alterations in the kidneys, including tubular dilation and epithelial sloughing, indicating enhanced tubular disintegration—especially affecting the proximal convoluted tubules and Bowman's capsule (Dosumu et al. 2021). Similarly, DMBA-induced breast cancer has been associated with elevated levels of kidney function biomarkers such as BUN and creatinine (Hendi et al. 2020), which is corroborated by the present study. Tumor-bearing mice exhibited significantly increased levels of BUN, uric acid, and creatinine, indicating renal impairment. Although abemaciclib administration has been associated with mild and variable elevations in serum creatinine, this may reflect a reduced glomerular filtration rate (GFR) and potential nephron injury (Chappell et al. 2019). In this study, abemaciclib-treated tumor mice exhibited a further increase in BUN, while changes in uric acid and creatinine levels were statistically insignificant compared with the control group, suggesting a mild but notable impact on renal function.

Previous studies have reported that DMBA-induced breast tumors increase oxidative stress by elevating lipid peroxidation products such as MDA, while reducing the levels of antioxidant enzymes such as CAT (Alanazy et al. 2021; Batcioglu et al. 2012). Consistent with these findings, the present study demonstrated that DMBA injection significantly elevated MDA levels and reduced CAT activity, likely due to overproduction of ROS which can damage cellular biomolecules and induce cytotoxicity.

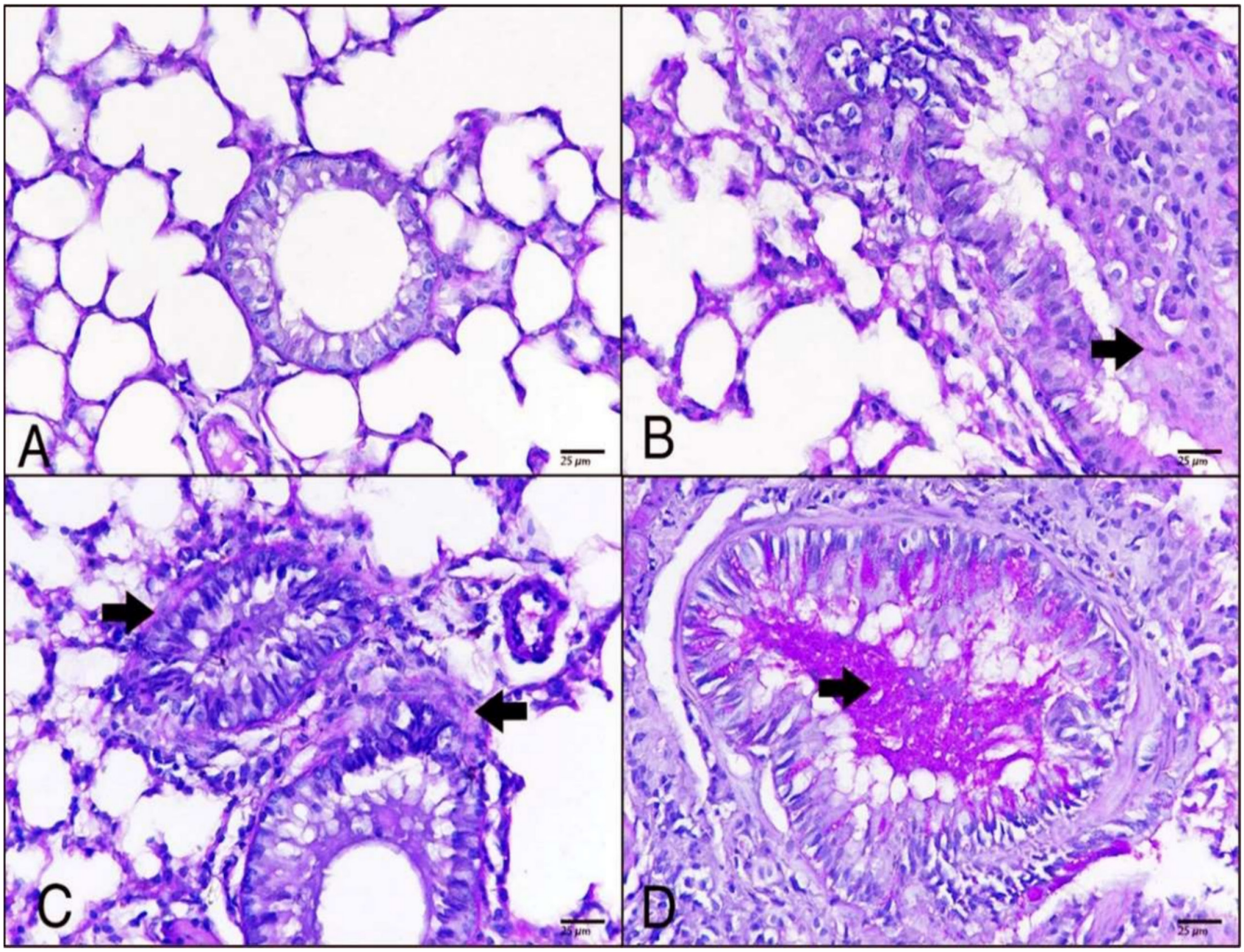

FIGURE 5 | Photomicrographs of mice lung stained with periodic acid Schiff. (A) untreated control lung showing no hyaline membranes, (B) lung treated with abemaciclib 50 mg/kg showing intense existence of hyaline membranes and mucus (black arrow), (C) lung of tumor group displaying hyaline membranes (black arrow), (D) lung of tumor group treated with abemaciclib 50 mg/kg showing high hyaline membranes (black arrow) (PAS—400×).

TABLE 2 | Effect of abemaciclib on the pathological scoring of lung induced by DMBA.

Group	Vascular alterations	Vascular and alveolar changes	Bronchiole alterations	Total score
Control	0	0	0	0
Abc 50	2	2	1	5
Tumor (DMBA)	2	3	2	7
T + Abc 50	3	2	3	8

Under physiological conditions, ROS such as hydroxyl radicals, superoxide anions, and hydrogen peroxide are generated during normal cellular processes and are neutralized by the body's antioxidant defense mechanisms (Mates 2000). However, the carcinogen DMBA induces excessive ROS generation and promotes lipid peroxidation. Chemical carcinogens like DMBA are known to stimulate ROS production through gene mutations, increased metabolic activity of tumor cells, and enhanced activity of oxidases, lipoxygenases, and cyclooxygenases (Perillo et al. 2020). Due to its high polyunsaturated fatty acid content, DMBA intensifies the lipid peroxidation process, further disrupting the cellular antioxidant defense system (Batcioglu et al. 2012).

Moreover, treatment with abemaciclib alone has also been associated with increased MDA levels and decreased CAT activity, possibly due to its role in enhancing lipid peroxidation and ROS production, thereby altering oxidative metabolism (Franco et al. 2016; Uçar et al. 2022). In the current study, mice treated with abemaciclib alone exhibited a significant increase in MDA levels and a decrease in CAT activity. Similarly, the tumor group treated with abemaciclib showed elevated MDA levels and reduced CAT activity, indicating a continued oxidative imbalance. Histopathologically, mammary carcinoma is characterized by nests and ribbons of invasive ductal adenocarcinoma composed of relatively large, pleomorphic, and atypical cells, often surrounded by a dense desmoplastic stroma rich in collagen fibers (Alghamdi et al. 2024). In this study, the DMBA-induced

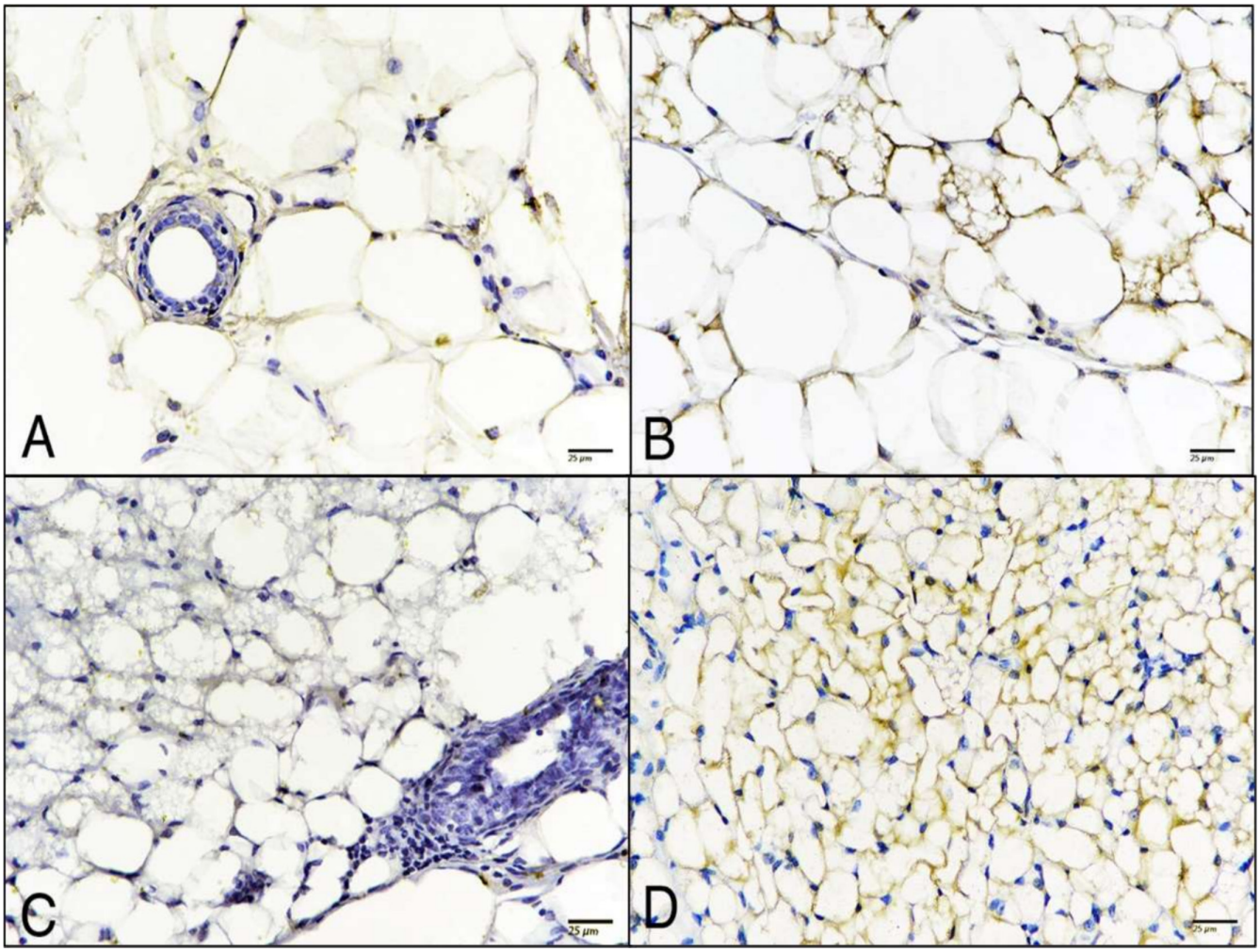

FIGURE 6 | Photomicrographs of breast tissue stained immunohistochemically for adiponectin expression. (A) Untreated control showing a strong immune response, (B) breast of treated mice with abemaciclib 50 mg/kg displaying strong immune response, (C) breast of tumor group revealing negative immune response, (D) breast of tumor group treated with abemaciclib 50 mg/kg showing increased immune response (ABC—400×).

tumor group exhibited mammary carcinoma with pleomorphic carcinoma cells arranged in nests and ribbons, along with high Nottingham histopathological scores and pronounced desmoplastic reactions. In contrast, the tumor group treated with abemaciclib displayed a noticeable reduction in carcinoma cell presence, lower histopathological scores, and diminished desmoplastic stromal response.

Mammary carcinoma induced by DMBA is often associated with generalized pathological changes in the lung. Intra-alveolar congestion and inflammatory infiltration are prominent features, with alveoli appearing swollen and filled with blood due to the prolonged action of DMBA. This alveolar swelling leads to increased tissue opacity and density, impairing normal lung function (Mannan et al. 2017). Consistent with these findings, the present study observed severe lung pathological alterations following a single DMBA dose, including intense inflammation, bronchial epithelial hyperplasia and dysplasia, along with marked accumulation of fibrosis, extracellular matrix components, and hyaline membranes. Administration of abemaciclib has also been reported to cause histopathological changes such as alveolar wall thickening, interstitial inflammation, and fibrosis, accompanied by infiltration of lymphocytes and macrophages (Mitarai et al. 2022). In agreement with this, the current study revealed that abemaciclib treatment further increased lung inflammation, collagenous fiber deposition, and accumulation of hyaline membranes and mucus—findings consistent with those reported by Mitarai and colleagues.

Adiponectin, an adipokine with anti-inflammatory and antitumorigenic properties, plays a critical role in suppressing breast tumorigenesis and mitigating various pathological conditions including inflammation and malignancy (Nehme et al. 2022). A meta-analysis by Gu et al. (2018), which included 31 studies, reported significantly lower circulating adiponectin levels in breast cancer patients, suggesting an inverse association between adiponectin levels and breast cancer risk. In the present study, the DMBA-induced tumor group exhibited reduced adiponectin expression, as demonstrated by immunohistochemistry, likely due to the high tumor burden. However, in the tumor group treated with abemaciclib, adiponectin expression was increased, which may be attributed to the drug's inhibitory effects on tumor progression and inflammation.

TNF-α is a multifunctional proinflammatory cytokine of the TNF superfamily that signals through two primary receptors:

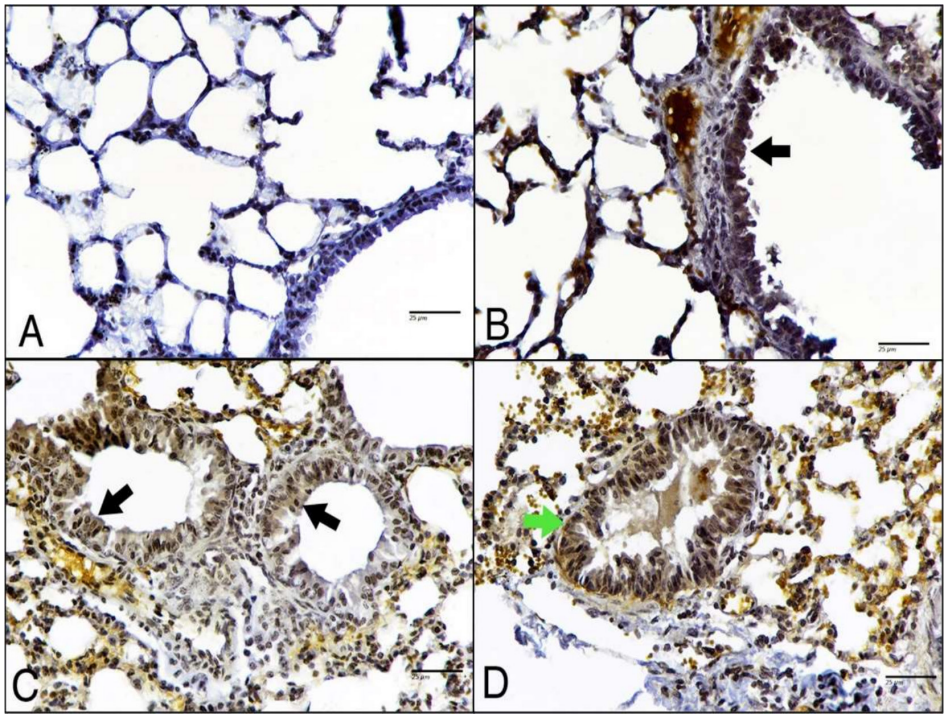

FIGURE 7 | Photomicrographs of lungs stained immunohistochemically against TNFα. (A) Untreated control showing a weak immune response, (B) lungs of treated mice with abemaciclib 50 mg/kg displaying strong immune response in columnar epithelia (black arrow), (C) lungs of tumor group revealing intense immune response (black arrow), (D) lungs of tumor group treated with abemaciclib 50 mg/kg showing intense immune response (green arrow) (ABC—400×).

TNFR1 and TNFR2. While the role of TNF-α in lung carcinogenesis remains unclear, chronic TNF-α production is believed to promote tumor development by facilitating tissue remodeling and stromal expansion necessary for tumor growth and metastasis (Arnott et al. 2002). Nadda et al. (2013) reported that TNF-α expression is significantly elevated in DMBA-induced tumor models, underscoring its role in inflammation and angiogenesis. The present study corroborates these findings, showing that DMBA-induced mammary carcinoma significantly elevated TNF-α expression, likely due to its involvement in inflammatory responses, immune modulation, and carcinogenic processes. Furthermore, abemaciclib treatment led to an additional increase in TNF-α expression, indicating a potential proinflammatory effect associated with the drug.

5 | Conclusion

Administration of DMBA to induce mammary carcinoma resulted in a high incidence of tumor formation, pronounced desmoplastic reactions, hormonal imbalances, liver injury, kidney damage, and elevated oxidative stress. DMBA exposure also led to severe pathological alterations in the lungs, characterized by increased inflammation and extracellular matrix accumulation. Treatment with abemaciclib significantly reduced mammary carcinoma incidence and desmoplastic stroma formation, in addition to partially modulating hormone levels. However, abemaciclib administration was associated with exacerbated liver and kidney damage, as well as heightened oxidative stress. Furthermore, lung tissues from abemaciclib-treated groups exhibited more severe pathological features, including blood clot formation and intensified inflammation. Therefore, although abemaciclib shows potential antitumor activity, its associated systemic toxicities warrant further investigation. Future research is necessary to better understand its safety profile and to explore strategies for minimizing its adverse effects.

Acknowledgments

The authors express their sincere appreciation to the Ongoing Research Funding Program ORF-2025-214, King Saud University, Riyadh, Saudi Arabia.

Ethics Statement

The study was approved by the Institutional Review Board (IRB), Committee of Ethics, King Saud University, Riyadh, Saudi Arabia (Approval No. KSU-SE-23-42), and followed international guidelines for animal studies.

Consent

The authors have nothing to report.

Conflicts of Interest

The authors declare no conflicts of interest.

Data Availability Statement

The datasets generated during and/or analyzed during the current study are available from the corresponding author upon reasonable request.

References

ACS. 2021. *Breast Cancer.* American Cancer Society. https://www.cancer.org/.

Alanazy, I. A., D. M. El-Naga, K. E. Ibrahim, A. M. Rady, and M. F. Khan. 2021. "Melatonin Abrogates Liver, Ovarian, and Uterine Toxicities Induced by Tamoxifen in a Breast Cancer Mouse Model." *Indian Journal of Experimental Biology* 59, no. 01: 33–43. https://doi.org/10.56042/ijeb.v59i01.44650.

Alghamdi, A., H. Alobaid, A. Rady, et al. 2024. "Inhibitory Effect of PD173074 Drug on DMBA-Induced Mammary Carcinoma in Female Swiss Albino Mice." *Tropical Journal of Pharmaceutical Research* 23, no. 12: 1983–1989. https://doi.org/10.4314/tjpr.v23i12.3.

Arnold, M., E. Morgan, H. Rumgay, et al. 2022. "Current and Future Burden of Breast Cancer: Global Statistics for 2020 and 2040." *Breast* 66: 15–23. https://doi.org/10.1016/j.breast.2022.08.010.

Arnott, C. H., K. A. Scott, R. J. Moore, et al. 2002. "Tumour Necrosis Factor-α Mediates Tumour Promotion via a PKCα-and AP-1-Dependent Pathway." *Oncogene* 21, no. 31: 4728–4738. https://doi.org/10.1038/sj.onc.1205588.

Batcioglu, K., A. B. Uyumlu, B. Satilmis, et al. 2012. "Oxidative Stress in the *In Vivo* DMBA Rat Model of Breast Cancer: Suppression by a Voltage-Gated Sodium Channel Inhibitor (RS 100642)." *Basic & Clinical Pharmacology & Toxicology* 111, no. 2: 137–141. https://doi.org/10.1111/j.1742-7843.2012.00880.x.

Buque, A., M. Perez-Lanzon, G. Petroni, et al. 2021. "MPA/DMBA-Driven Mammary Carcinomas." In *Methods in Cell Biology*, vol. 163, 1–19. Academic Press. https://doi.org/10.1016/bs.mcb.2020.08.003.

Cakcak, I. E., Y. E. Aytin, S. Sayin, et al. 2023. "An Experimental Study: The Effect of *S. boulardii* on Abemaciclib-Induced Diarrhea." *Turkish Journal of Medical Sciences* 53, no. 1: 51–57. https://doi.org/10.55730/1300-0144.5557.

Chappell, J. C., P. K. Turner, Y. A. Pak, et al. 2019. "Abemaciclib Inhibits Renal Tubular Secretion Without Changing Glomerular Filtration Rate." *Clinical Pharmacology and Therapeutics* 105, no. 5: 1187–1195. https://doi.org/10.1002/cpt.1296.

Corona, S. P., and D. Generali. 2018. "Abemaciclib: A CDK4/6 Inhibitor for the Treatment of HR+/HER2− Advanced Breast Cancer." *Drug Design, Development and Therapy* 12: 321–330. https://doi.org/10.2147/DDDT.S137783.

Corso, C. R., and A. Acco. 2018. "Glutathione System in Animal Model of Solid Tumors: From Regulation to Therapeutic Target." *Critical Reviews in Oncology/Hematology* 128: 43–57. https://doi.org/10.1016/j.critrevonc.2018.05.014.

CRUK. 2023. *About Breast Cancer Staging and Grades*. Cancer Research UK. https://www.cancerresearchuk.org/.

Dakrory, A. I., S. R. Fahmy, A. M. Soliman, A. S. Mohamed, and S. A. Amer. 2015. "Protective and Curative Effects of the Sea Cucumber *Holothuria atra* Extract Against DMBA-Induced Hepatorenal Diseases in Rats." *BioMed Research International* 1: 563652. https://doi.org/10.1155/2015/563652.

Dosumu, O. A., A. I. Bababode, S. O. Rotimi, et al. 2021. "DMBA-Induced Kidney Dysfunction: Effects of Supplementary Dietary Vitamin K in Rats." *Tropical Journal of Natural Product Research* 5: 917–923. https://doi.org/10.26538/tjnpr/v5i5.19.

Duro de Oliveira, K., M. Vannucci Tedardi, B. Cogliati, and M. L. Zaidan Dagli. 2013. "Higher Incidence of Lung Adenocarcinomas Induced by DMBA in Connexin 43 Heterozygous Knockout Mice." *BioMed Research International* 2013, no. 1: 618475. https://doi.org/10.1155/2013/618475.

Food and Drug Administration, FDA Approves Abemaciclib With Endocrine Therapy for Early Breast Cancer. Media Release. 2021.

Franco, J., U. Balaji, E. Freinkman, A. K. Witkiewicz, and E. S. Knudsen. 2016. "Metabolic Reprogramming of Pancreatic Cancer Mediated by CDK4/6 Inhibition Elicits Unique Vulnerabilities." *Cell Reports* 14, no. 5: 979–990. https://doi.org/10.1016/j.celrep.2015.12.094.

Gu, L., C. Cao, J. Fu, Q. Li, D. H. Li, and M. Y. Chen. 2018. "Serum Adiponectin in Breast Cancer: A Meta-analysis." *Medicine* 97, no. 29: e11433. https://doi.org/10.1097/MD.0000000000011433.

Hamza, A. A., M. A. Khasawneh, H. M. Elwy, S. O. Hassanin, S. F. Elhabal, and N. M. Fawzi. 2022. "*Salvadora persica* Attenuates DMBA-Induced Mammary Cancer Through Downregulation Oxidative Stress, Estrogen Receptor Expression and Proliferation and Augmenting Apoptosis." *Biomedicine & Pharmacotherapy* 147: 112666. https://doi.org/10.1016/j.biopha.2022.112666.

Hassanpour, S. H., and M. Dehghani. 2017. "Review of Cancer From Perspective of Molecular." *Journal of Cancer Research and Practice* 4, no. 4: 127–129. https://doi.org/10.1016/j.jcrpr.2017.07.001.

Hendi, A. A., D. M. El-Nagar, M. A. Awad, K. M. Ortashi, R. A. Alnamlah, and N. M. Merghani. 2020. "Green Nanogold Activity in Experimental Breast Carcinoma In Vivo." *Bioscience Reports* 40, no. 11: BSR20200115.

Huang, J., L. Zheng, Z. Sun, and J. Li. 2022. "CDK4/6 Inhibitor Resistance Mechanisms and Treatment Strategies." *International Journal of Molecular Medicine* 50, no. 4: 128. https://doi.org/10.3892/ijmm.2022.5184.

Ma, Z., Y. M. Kim, E. W. Howard, et al. 2018. "DMBA Promotes ErbB2-Mediated Carcinogenesis via ErbB2 and Estrogen Receptor Pathway Activation and Genomic Instability." *Oncology Reports* 40, no. 3: 1632–1640. https://doi.org/10.3892/or.2018.6545.

Mannan, R., R. Arora, S. BhuShAn, S. ShARMA, T. Bhasin, and S. Arora. 2017. "Bioprotective Efficacy of Erucin Against 7, 12-Dimethylbenz (α) Anthracene-Induced Microstructural Changes in Male Wistar Rats." *Turkish Journal of Pathology* 33: 150–156. https://doi.org/10.5146/tjpath.2016.01381.

Mates, J. M. 2000. "Effects of Antioxidant Enzymes in the Molecular Control of Reactive Oxygen Species Toxicology." *Toxicology* 153, no. 1–3: 83–104. https://doi.org/10.1016/s0300-483x(00)00306-1.

Mitarai, Y., Y. Tsubata, and M. Hyakudomi. 2022. "Drug-Induced Eosinophilic Pneumonia as an Adverse Event of Abemaciclib." *Cureus.* 14, no. 1: e21741. https://doi.org/10.7759/cureus.21741.

Momenimovahed, Z., and H. Salehiniya. 2019. "Epidemiological Characteristics of and Risk Factors for Breast Cancer in the World." *Breast Cancer: Targets and Therapy* 11: 151–164. https://doi.org/10.2147/BCTT.S176070.

Nadda, N., S. Setia, V. Vaish, and S. N. Sanyal. 2013. "Role of Cytokines in Experimentally Induced Lung Cancer and Chemoprevention by COX-2 Selective Inhibitor, Etoricoxib." *Molecular and Cellular Biochemistry* 372, no. 1: 101–112. https://doi.org/10.1007/s11010-012-1451-3.

NCI 2022 Abemaciclib https://www.cancer.gov/about-cancer/treatment/drugs/abemaciclib.

Nehme, R., M. Diab-Assaf, C. Decombat, L. Delort, and F. Caldefie-Chezet. 2022. "Targeting Adiponectin in Breast Cancer." *Biomedicine* 10, no. 11: 2958. https://doi.org/10.3390/biomedicines10112958.

Passmore, M. R., L. Byrne, N. G. Obonyo, et al. 2018. "Inflammation and Lung Injury in an Ovine Model of Fluid Resuscitated Endotoxemic Shock." *Respiratory Research* 19, no. 1: 231. https://doi.org/10.1186/s12931-018-0935-4.

Patel, P., and J. Shah. 2021. "Protective Effects of Hesperidin Through Attenuation of Ki67 Expression Against DMBA-Induced Breast Cancer in Female Rats." *Life Sciences* 285: 119957. https://doi.org/10.1016/j.lfs.2021.119957.

Perillo, B., M. Di Donato, A. Pezone, et al. 2020. "ROS in Cancer Therapy: The Bright Side of the Moon." *Experimental & Molecular Medicine* 52, no. 2: 192–203. https://doi.org/10.1038/s12276-020-0384-2.

Royce, M., C. Osgood, F. Mulkey, et al. 2022. "FDA Approval Summary: Abemaciclib With Endocrine Therapy for High-Risk Early Breast

Cancer." *Journal of Clinical Oncology* 40, no. 11: 1155–1162. https://doi.org/10.1200/JCO.21.02742.

Takahashi, H., M. Oshi, M. Asaoka, L. Yan, I. Endo, and K. Takabe. 2020. "Molecular Biological Features of Nottingham Histological Grade 3 Breast Cancers." *Annals of Surgical Oncology* 27, no. 11: 4475–4485. https://doi.org/10.1245/s10434-020-08608-1.

Taniguchi, A., N. Kittaka, H. Kanaoka, et al. 2022. "Risk of Abemaciclib-Induced Liver Injury in Hormone Receptor-Positive, HER2-Negative Metastatic Breast Cancer: A Retrospective Analysis." *Anticancer Research* 42, no. 12: 6027–6035. https://doi.org/10.21873/anticanres.16114.

Uçar, B., Z. Huyut, F. Altındağ, Ö. F. Keleş, and K. Yıldızhan. 2022. "Relationship With Nephrotoxicity of Abemaciclib in Rats: Protective Effect of Curcumin." *Indian Journal of Biochemistry & Biophysics* 59, no. 10: 963–976. https://doi.org/10.56042/ijbb.v59i10.64336.

Supporting Information

Additional supporting information can be found online in the Supporting Information section. **Figure S1:** Bar chart showing the effect of Abemaciclib (50 mg/kg, oral, daily) on mammary and lung indices in DMBA-induced tumor-bearing mice. (A) Breast index and (B) lung index were calculated as organ weight/body weight × 100. Data are presented as mean ± SEM ($n = 10$ per group). Statistical significance was assessed using one-way ANOVA followed by Tukey's post hoc test, with $p < 0.05$ considered significant. **Figure S2:** Bar chart showing the effect of Abemaciclib (50 mg/kg, oral, daily) on serum female hormone levels in DMBA-induced tumor-bearing mice. (A) Estrogen and (B) Progesterone concentrations were measured using ELISA. Data are presented as mean ± SEM (n = 10 per group). Statistical significance was evaluated by one-way ANOVA followed by Tukey's post hoc test, with $p < 0.05$ considered significant. **Figure S3:** Bar chart showing the effect of Abemaciclib (50 mg/kg, oral, daily) on hepatic enzyme activities in DMBA-induced tumor-bearing mice. (A) ALT, (B) AST, and (C) ALP activities were measured in liver homogenates using standard biochemical assay kits. Data are presented as mean ± SEM (n = 10 per group). Statistical significance was determined by oneway ANOVA followed by Tukey's post hoc test, with $p < 0.05$ considered significant. **Figure S4:** Bar chart showing the effect of Abemaciclib (50 mg/kg, oral, daily) on kidney function markers in DMBA-induced tumor-bearing mice. (A) Uric acid, (B) Urea, and (C) Creatinine levels were measured in serum using standard biochemical assay kits. Data are presented as mean ± SEM (n = 10 per group). Statistical significance was determined by one-way ANOVA followed by Tukey's post hoc test, with $p < 0.05$ considered significant. **Figure S5:** Bar chart showing the effect of Abemaciclib (50 mg/kg, oral, daily) on oxidative stress markers in DMBA-induced tumor-bearing mice. (A) Malondialdehyde (MDA) levels and (B) Catalase (CAT) activity were measured in liver homogenates using standard biochemical assay kits. Data are presented as mean ± SEM (n = 10 per group). Statistical significance was determined by one-way ANOVA followed by Tukey's post hoc test, with $p < 0.05$ considered significant. **Figure S6:** Bar chart showing the effect of Abemaciclib (50 mg/kg, oral, daily) on Masson's trichrome staining in breast tissue of DMBA-induced tumor-bearing mice. (A) Percentage area (%) and (B) optical density (OD) of Masson's trichrome staining were quantified using Fiji software. Data are presented as mean ± SEM (n = 10 per group). Statistical significance was determined by one-way ANOVA followed by Tukey's post hoc test, with $p < 0.05$ considered significant. **Figure S7:** Bar chart showing the effect of Abemaciclib (50 mg/kg, oral, daily) on Masson's trichrome staining in lung tissue of DMBA-induced tumor-bearing mice. (A) Percentage area (%) and (B) optical density (OD) of staining were quantified using Fiji software. Data are presented as mean ± SEM (n = 10 per group). Statistical significance was determined by one-way ANOVA followed by Tukey's post hoc test, with $p < 0.05$ considered significant. **Figure S8:** Bar chart showing the effect of Abemaciclib (50 mg/kg, oral, daily) on PAS staining in lung tissue of DMBA-induced tumor-bearing mice. (A) Percentage area (%) and (B) optical density (OD) were quantified using Fiji software. Data are presented as mean ± SEM (n = 10 per group). Statistical significance was determined by one-way ANOVA followed by Tukey's post hoc test, with $p < 0.05$ considered significant. **Figure S9:** Bar chart showing the effect of Abemaciclib (50 mg/kg, oral, daily) on the immune response in breast tissue of DMBA-induced tumor-bearing mice against Adiponectin (ADIPOQ). (A) Percentage area (%) and (B) optical density (OD) of Adiponectin staining were quantified using Fiji software. Data are presented as mean ± SEM (n = 10 per group). Statistical significance was determined by one-way ANOVA followed by Tukey's post hoc test, with $p < 0.05$ considered significant. **Figure S10:** Bar chart showing the effect of Abemaciclib (50 mg/kg, oral, daily) on the immune response in lung tissue of DMBA-induced tumor-bearing mice against TNFα. (A) Percentage area (%) and (B) optical density (OD) of TNFα staining were quantified using Fiji software. Data are presented as mean ± SEM (n = 10 per group). Statistical significance was determined by one-way ANOVA followed by Tukey's post hoc test, with $p < 0.05$ considered significant.